A&A manuscript no.
(will be inserted by hand later)

Your thesaurus codes are:
03(11.17.4 B1152+199; 11.09.4; 09.04.1; 09.05.1; 12.07.1)

ASTRONOMY
AND
ASTROPHYSICS

The extinction curve of the lensing galaxy of B1152+199 at $z = 0.44^\star$

Sune Toft[1], **Jens Hjorth**[1], **and Ingunn Burud**[2]

[1] Astronomical Observatory, University of Copenhagen, Juliane Maries Vej 30, DK–2100 Copenhagen Ø, Denmark
[2] Institut d'Astrophysique et de Géophysique, Université de Liège, Avenue de Cointe 5, B–4000 Liège, Belgium

the date of receipt and acceptance should be inserted later

Abstract. We present $UBVRIz'$ photometry of the gravitational lens candidate CLASS B1152+119 obtained with the Nordic Optical Telescope. The two QSO components are resolved in the B, V, R, I and z' bands confirming the lensing nature of the system. The $z = 0.44$ lens galaxy is clearly detected in B, R, I and z' and its position is found to be almost coincident with the faint QSO image which is heavily extincted (relative to the brighter QSO image) by dust in the lens galaxy. The extinction curve of the lens galaxy derived from the relative photometry is well fitted by a Galactic extinction law with $1.3 \lesssim R_V \lesssim 2.0$ and $E(B-V) \approx 1$. From a simple model of the system we predict a time delay of ~ 60 days.

Key words: quasars: individual: B1152+199 – galaxies: ISM – ISM: dust, extinction – ISM: evolution – gravitational lensing

1. Introduction

Dust is ubiquitous in the Universe and is responsible for extinction of the light from distant sources. The type of dust (composition, grain sizes and shape) determines the amount of extinction as a function of wavelength – the extinction curve A_λ. Extinction curves almost certainly evolve with redshift since the metallicity, elemental abundance ratios, mean star-formation rate, and energy-injection rates that determine the structure and evolution of the dust are all strong functions of redshift. The extinction in our Galaxy has been well studied (Cardelli et al. 1989), but very little is known about extinction in other galaxies, especially at higher redshifts. This is unfortunate as dust plays an increasingly important role in contemporary cosmology.

Recently the use of multiply imaged QSOs has been explored as a means of inferring differential extinction curves for distant galaxies (Nadeau et al. 1991; Malhotra et al. 1997; Falco et al. 1999). The idea behind this approach is that a lensed QSO can be used as a 'standard beacon', shining through different paths of the lensing galaxy. If one of the images suffers negligible extinction, or if the extinction curve is the same throughout the galaxy, then the relative intensity ratios of any two images as a function of wavelength is a direct measure of the extinction curve.

As a part of the CLASS radio survey, Myers et al. (1999) reported the discovery of a new gravitational lens candidate, CLASS B1152+199, with an image separation of $\theta = 1\farcs56$ and a flux ratio of 3.03 ± 0.03 at 8.46 GHz. Spectra obtained with the Keck II telescope revealed a background quasar at $z = 1.019$ and a foreground galaxy at $z = 0.439$. Optical follow-up observations revealed a bright unresolved object ($g \simeq 16.5$ and $i \simeq 16.6$) located at the radio position, presumably the brighter of the two lensed images. The non-detection of the weak image in g and i is indicative of a large color difference between the two images. If B1152+199 is indeed a gravitationally lensed system this could be attributed to differential extinction caused by dust in the lens, making B1152+199 a well-suited system for studying the extinction law of the lensing galaxy.

2. Observations and reduction

We have performed multiwavelength $UBVRIz'$ photometry on data of B1152+199 obtained with the ALFOSC instrument at the 2.56-m Nordic Optical Telescope (NOT). The ALFOSC instrument is equipped with a Loral/Lesser CCD with an approximate gain of $q = 1\,e^-/\mathrm{ADU}$ and $\mathrm{RON} = 6\,\mathrm{e}^-/\mathrm{pixel}$ and a pixel scale of $0\farcs188$/pixel. The observations were performed within the span of a few days to avoid time delay and variability effects. The observing log is given in Table 1. The conditions were photometric with average seeing ranging from $0\farcs8$ in the z' band to $1\farcs3$ in the U band. The CCD frames were reduced (overscan

* Nordic Optical Telescope is operated on the island of La Palma jointly by Denmark, Finland, Iceland, Norway, and Sweden, in the Spanish Observatorio del Roque de los Muchachos of the Instituto de Astrofisica de Canarias.

Date	U	B	V	R	I	z'
UT	sec	sec	sec	sec	sec	sec
June 23 1999				600	600	
June 25 1999	2700	1100	400			900
July 02 1999		400	600			

Table 1. Observing log giving the dates of observation and the total exposure times for each night

subtracted, trimmed and flatfielded) using an IRAF-based pipeline.[1]

On June 25 1999 UT, we also obtained photometric $UBVRI$ observations of standard stars in M92. Using these and calibrated photometry by Davis (private communication) we fitted the transformation equations to 19 stars in M92 to derive the color, extinction and zero-point terms for the calibration to the Johnson–Kron–Cousins system.

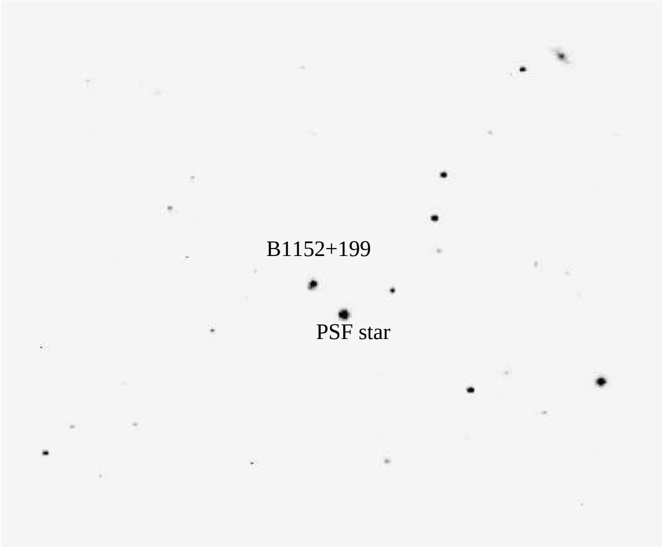

Fig. 1. $160'' \times 140''$ finding chart for B1152+119. North is up, East is to the left. The star used to model the point-spread function is indicated

3. Deconvolution of B1152+199

The two QSO images together with the lens galaxy were deconvolved with the MCS deconvolution algorithm (Magain et al. 1998). This method is based on the principle that the resolution of a deconvolved image must be compatible with its sampling, which is limited by the Nyquist frequency. In order to improve the sampling of the images we adopted a pixel size in the deconvolved images as half the pixel size of the original frames ($0\farcs188/2 = 0\farcs094$). (See Burud et al. 1998 for more details on the implementation of the MCS algorithm).

In order to successfully deconvolve the images, the point-spread function (PSF) must be bright and located close to B1152+199 to minimize the photon noise and to avoid PSF variation as a function of the position on the chip. We used the bright star $13''$ South West of B1152+199 as a PSF star (Fig. 1). Careful examination revealed that this star had a faint red companion. By deconvolving this star with another PSF in the field we were able to resolve the red companion star and subtract it, before using the bright star as a model for the PSF. We compared the star to other stars in the field to check that the companion star was correctly subtracted. The best fitting positions of the weak QSO image relative to the strong QSO image returned from the MCS algorithm is given in Table 2. These yield a smaller separation that expected from the radio positions (Myers et al. 1999). The deconvolution code is very sensitive to PSF variations, and small residuals from the subtraction of the red companion could explain the discrepancies between the fitted positions and the radio position of the weak QSO image.

In order to improve the photometry we fixed the position of the weak QSO image relative to the bright QSO image to the radio coordinates. The quality of the results was checked from the residual maps, as explained by Courbin et al. (1998). During the deconvolution the lens galaxy can be modeled numerically or by an analytical function (e.g., de Vaucouleurs, exponential-disk law). The lens galaxy in B1152+199 was well fitted by the numerical model and an exponential disk law, whereas a de Vaucouleurs model gave significantly bad residuals. The best fitting exponential disk law was centered at $(\Delta\alpha, \Delta\delta) = (0\farcs29 \pm 0\farcs02, -0\farcs89 \pm 0\farcs04)$ relative to the bright QSO image.

Both components of B1152+199 were resolved in the V, R, I and z' bands (Fig. 2). Following Myers et al. (1999) we will refer to the bright component as "A" and the weak component as "B". In the U and B bands we failed to detect the B image due to the increasing size of the seeing disc with shorter wavelength and the large differential extinction of the system (see Sect. 5). The lens galaxy was detected in the R, I and z' bands. We performed aperture photometry of the galaxy on the deconvolved images with an aperture diameter of $2\farcs26$. The U, B, V, R and I band magnitudes of the A and B images and the galaxy (G) were calibrated (Table 3) whereas no standard photometry was available in the z' band.

Additional extended signal was observed just South East of the B image (notably in the I band). We discuss this further in Sect. 4.

4. PSF photometry of B1152+199

In addition to the deconvolution we performed PSF photometry on the system with the IRAF DAOPHOT package (Stetson 1987). As PSF star we used the same star

[1] developed by Andreas O. Jaunsen

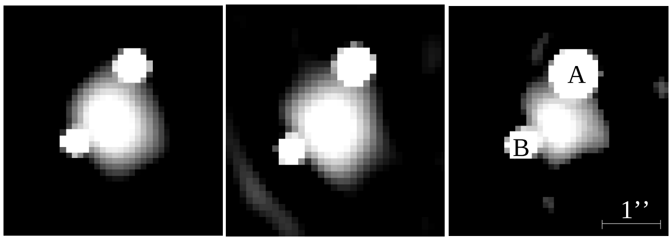

Fig. 2. Deconvolved images of B1152+199 in the (from left to right) z', R and I bands. The resolution (FWHM) is $0\farcs28$ in the R band image and $0\farcs19$ in the I and z' band images. The bright QSO component is labeled "A" and the faint component is labeled "B"

as in the deconvolution, with the faint red companion removed with the IRAF task substar. Again we fixed the position of the B image relative to the A image on the the radio position to ensure the correct separation. The results from this analysis is not as robust as the results from the deconvolution since it does not simultaneously fit a model for the galaxy, but the differences between the results of the two approaches is indicative of the magnitude of the systematic photometric uncertainties.

The two QSO images were resolved in the B, V, R, I and z' bands. The results from the PSF photometry is given in Table 2. After subtracting the scaled PSFs we detected the lensing galaxy in the B, R, I and z' band residual images (Fig. 3). The I and z' band images indicates that the extended flux South East of the B image, detected in the deconvolved images, stems from the lensing galaxy. The light from the B component passes through the galaxy close to its center, and in the deconvolution process some of the light from the galaxy may have been attributed to the B image.

To test the results from the deconvolution we performed aperture photometry with the SExtracter software (Bertin & Arnouts 1996) on the images cleaned with DAOPHOT. The residual images in Fig. 3 show artifacts of the PSF subtraction (seen as circular dark spots). These affect the aperture photometry which should therefore be considered rather uncertain. In the I and B bands we obtain $I = 19.43 \pm 0.03$ and $B = 20.24 \pm 0.02$ with an aperture diameter of $2\farcs26$. In the R band the signal is rather weak, and thus in the outer parts dominated by the PSF subtraction artifacts. We can however obtain a color by comparing the R and I flux within an aperture of $1\farcs13$. This yields $R - I = 0.80 \pm 0.05$. The color of the galaxy from the deconvolution $(R-I)_{\rm MCS} = 0.43 \pm 0.06$ or from PSF photometry $(R-I)_{\rm PSF} = 0.80 \pm 0.05$ are consistent with the lensing galaxy being a irregular or late type galaxy at $z = 0.439$ (Fukugita et al. 1995). By comparing the photometric results from the two approaches we estimate the magnitude of the systematic photometric errors due to the limited quality of the data to be in the order of 0.4 mag for galaxy magnitudes and 0.2 mag for the QSO magnitudes.

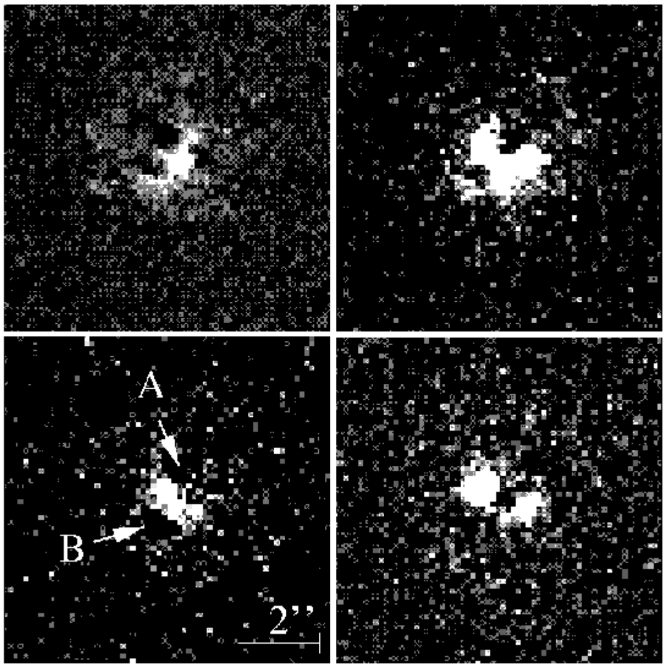

Fig. 3. PSF-subtracted z' (top left), I (top right), R (bottom left), and B (bottom right) images

Filter	$(B-A)_{\rm MCS}$ mag	$\Delta\alpha$ $''$	$\Delta\delta$ $''$	$(B-A)_{\rm PSF}$ mag
B				5.84 ± 0.51
V	4.42 ± 0.02	0.88	-1.19	4.44 ± 0.12
R	3.87 ± 0.06	0.78	-1.29	3.67 ± 0.06
I	2.98 ± 0.01	0.86	-1.22	2.69 ± 0.03
z'	2.61 ± 0.04	0.94	-1.20	2.29 ± 0.04

Table 2. Columns 2–4 give the flux ratios and astrometry for B1152+199 from the deconvolution. $\Delta\alpha$ and $\Delta\delta$ are the fitted positions of the B image relative to the A image. The rms uncertainties in the positions are approximately $0\farcs05$ in $\Delta\alpha$ and $0\farcs01$ in $\Delta\delta$. The positions agree reasonably well with the radio positions $(\Delta\alpha, \Delta\delta) = (0\farcs935 \pm 0\farcs005, -1\farcs248 \pm 0\farcs005)$, although the separation is slightly smaller. This is a well-known effect due to the entanglement of the B image and galaxy flux. Column 5 gives the flux ratios from the PSF photometry

5. Galaxy extinction

Significant differential extinction of the B image relative to the A image was observed (Tables 2 and 3). The A image, however, does not appear to be significantly reddened. In what follows we assume that the A image is unaffected by extinction by dust in the lensing galaxy. The Galactic extinction curve is fairly well known, with A_λ well parameterized as a function of a single parameter, R_V, defined as the ratio between the V extinction, A_V, and the color index $E(B-V)$ (Cardelli et al. 1989; Fitzpatrick 1999).

	FWHM	A	B	G
U	$1\overset{''}{.}22$	16.75±0.04		
B	$1\overset{''}{.}09$	17.00±0.02		
V	$1\overset{''}{.}02$	17.28±0.03	21.73 ± 0.03	
R	$1\overset{''}{.}00$	16.42±0.02	20.20 ± 0.04	19.61 ± 0.04
I	$0\overset{''}{.}94$	16.38±0.02	19.26 ± 0.03	19.18 ± 0.04
z'	$0\overset{''}{.}83$			

Table 3. Photometry (mag) of image A, B and the lensing galaxy. The uncertainties are 1σ standard deviations, including standard-star zero point, calibration and photometry uncertainties

This parameterization is valid over the observed R_V values ranging from 2.5 to 6, with a mean (canonical) Galactic value of $R_V = 3.1$. Large R_V give flat UV extinction curves due to large grains whereas small R_V and small grains lead to large UV extinctions.

The variation of the flux ratio with wavelength directly measures the extinction curve of the galaxy. We have assumed that the intrinsic flux ratio is given by the radio flux ratio (B−A=1.21).

The extinction curve of B1152+199 was well fitted by a Galactic extinction law, using either the flux ratios from the deconvolution or from the PSF photometry. However the best fitting values of the parameters R_V and $E(B-V)$ differ somewhat. We first discuss the fit to the deconvolution data. In the deconvolved U and B band images the galaxy and the B image were too weak to be separated. We can however obtain upper limits on the B image flux by using the total flux of the galaxy and the B image. These are $B_{\rm galaxy+B} = 20.37$ and $U_{\rm galaxy+B} = 20.45$. The best fitting restframe values of the parameters to the deconvolution flux ratios are $R_V = 2.04\pm0.04$ and $E(B-V) = 0.89\pm0.02$ (Fig. 4, solid curve). The predicted magnitude of the B image from the observed A image magnitude and $R_V = 2.04$ are $B_{\rm B} = 21.69$ and $U_{\rm B} = 23.27$. Furthermore the inferred $B_{\rm galaxy+B}$ agree well with the B band magnitude of the galaxy inferred from the PSF photometry (Sect. 4). It is therefore likely that the upper limits presented above are dominated by the galaxy flux rather than flux from the B image.

The PSF photometry detected the B component in the B band which gives us another point on the extinction curve. The best fitting restframe values of the parameters to the PSF photometry flux ratios are $R_V = 1.32 \pm 0.02$ and $E(B-V) = 1.13 \pm 0.01$ (Fig. 4, dashed curve). The extinction curves inferred from the two approaches are comparable. As discussed in Sect. 4 the systematic uncertainties in the photometry is of the order 0.2 magnitudes. This uncertainty is illustrated by the different slopes of the extinction curves derived from the two approaches. We conclude that the extinction curve of the lensing galaxy of B1152+199 is fitted by the Galactic extinction law and put the following constrains on the parameters: $1.3 \lesssim R_V \lesssim 2.1$ and $0.9 \lesssim E(B-V) \lesssim 1.1$.

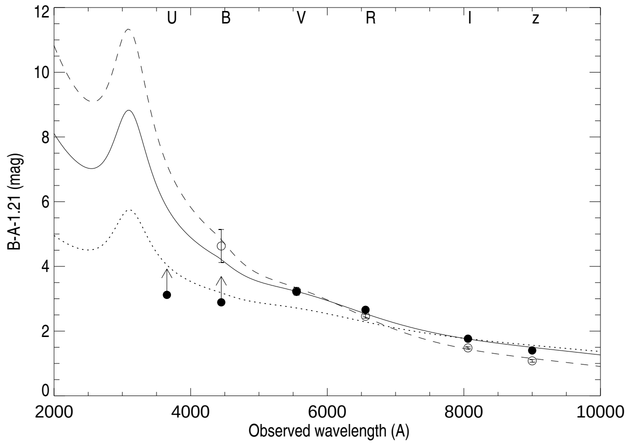

Fig. 4. Extinction curve of the lensing galaxy of B1152+199, fitted by a Galactic extinction law. The best fitting parameters to the deconvolution data (filled symbols) are $R_V = 2.04\pm0.04$ and $E(B-V) = 0.89 \pm 0.02$ (solid curve). The U and B band points are lower limits (see text). The best fitting parameters to the PSF photometry data (open symbols) are $R_V = 1.32\pm0.02$ and $E(B-V) = 1.13 \pm 0.01$ (dashed curve). For comparison we have overplotted the Galactic ($R_V = 3.1$) extinction curve (dotted curve)

$\Delta\alpha$	$\Delta\delta$	e	P.A.	$r_{\rm core}$	$r_{\rm cut}$	σ	delay
$''$	$''$	1−b/a	deg	kpc	kpc	km/s	days
0.56	−0.87	0.21	21	0.02	5.42	253	59

Table 4. Simple lens model parameters for B1152+199 (cf. Fig. 5). $\Delta\alpha$, $\Delta\delta$ are the positions of the lensing galaxy relative to the A component. The position of the galaxy and the QSO images along with their flux ratios were held constant in the fitting procedure, while the time delay was calculated from the best fit to the remaining parameters. $\Omega = 0.2$, $\Lambda = 0$, $H_0 = 65$ km s^{-1} Mpc^{-1} were assumed

If the reddening is due to dust extinction in the lens galaxy we can derive the column density of neutral hydrogen from the observed $E(B-V)$ by assuming a gas to dust ratio for the galaxy. For the Milky Way $\langle {\rm N(H\,I)/E(B-V)} \rangle_{\rm MW} = 4.93\times10^{21}$ cm^{-2} mag^{-1}, (Diplas & Savage 1994) while the value for Damped Lymanα Absorbers (DLAs) may be up to 20 times larger (Fall & Pei 1993). With the inferred $E(B-V) \approx 1$ for the lens galaxy: ${\rm N(H\,I)_{B1152+199}} = {\rm k} \times 10^{21}$ cm^{-2}, where $5 \lesssim k \lesssim 100$ is the parameterization of the range in the observed $\langle {\rm N(H\,I)/E(B-V)} \rangle$ in different systems. Thus, the lensing galaxy of B1152+199 would qualify as a DLA (${\rm N(H\,I)} > 2 \times 10^{20}$ cm^{-2}) regardless of the value of k.

6. A simple model of B1152+199

A simple model with a dark halo, represented by
$$\Sigma(R) = \Sigma_0 \frac{r_{\rm core} r_{\rm cut}}{r_{\rm cut} - r_{\rm core}} \left(\frac{1}{(r_{\rm core}^2 + R^2)} - \frac{1}{(r_{cut}^2 + R^2)} \right),$$

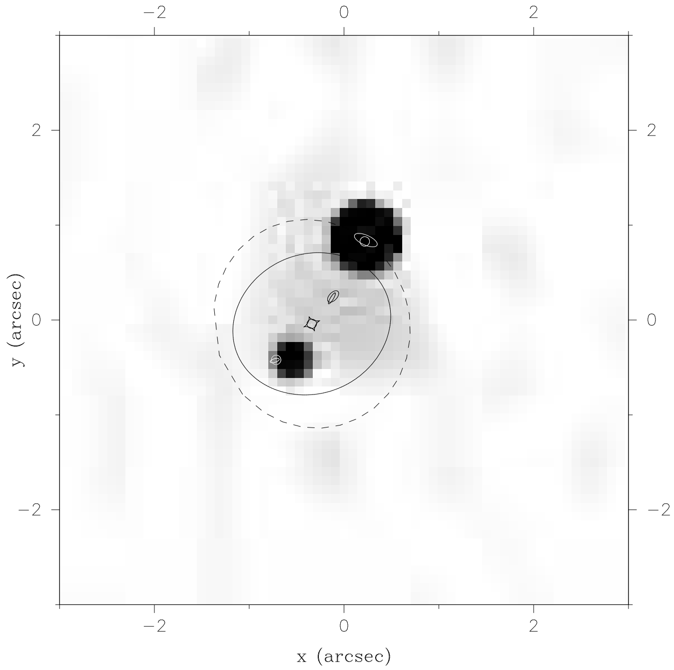

Fig. 5. Critical (solid) and caustic (dashed) curves from the model, overlaid the deconvolved R image

as the dominating mass was fitted to the data (Kneib et al. 1996). Although the observational constraints available from our data were too poor to perform detailed modeling, a set of best-fitting parameters could be derived for the system (see Table 5). We used the radio positions and flux ratios for the two QSO components while we experimented with different positions for the lens galaxy. We found that the two-image configuration could not be reproduced with the galaxy in the position found from the deconvolved images. An improved fit was obtained by placing the galaxy closer to the B component. The position was chosen to be consistent with what is found in the PSF-subtracted images. This position means that the B component passes through the galaxy while the A component passes outside the galaxy, which is consistent with the large observed differential extinction. The model predicts a time delay of 59 days. In Fig. 5 we show the critical and caustic curves of the lens model overlaid the deconvolved R image.

7. Discussion

Extinction curves have been derived for the Galaxy and the Magellanic Clouds, mainly through multi-color photometry of individual stars, for which the intrinsic luminosities is known from their spectral types (Cardelli et al. 1989). The extinction curves of the LMC and SMC can be fitted by the Galactic extinction law (see Mathis 1990; Fitzpatrick 1999). The main difference is the 2175 Å bump (cf. Fig. 4) which is not observed in the LMC and SMC. At distances $\gtrsim$ 10 Mpc study of individual stars is difficult and other methods must be considered. In this paper we have shown that accurate extinction curves of high-z galaxies can be determined by studying gravitationally lensed systems. We have found that the extinction curve of B1152+199 is well fitted by the Galactic extinction law. It is interesting to note that the inferred $1.3 \lesssim R_V \lesssim 2.1$ in principle is outside the validity of the parameterization of Galactic extinction curve by Cardelli et al. (1989). Note also that the differential extinction of B1152+199 $0.9 \lesssim E(B-V) \lesssim 1.1$, is one of the largest observed to date (Falco et al. 1999).

The evidence for a Galactic extinction curve is intriguing, but U and B band observations with longer exposure times and better seeing are needed to rule out other extinction curves. These will sample the restframe UV radiation which is highly sensitive to dust extinction, and thus strongly constrain the shape of the extinction curve, and allow for the possible detection of the 2175 Å bump.

The predicted time delay of 59 days makes B1152+199 an interesting candidate for monitoring.

Acknowledgements. We thank Andreas O. Jaunsen for providing the pipeline for the reduction, Jean-Paul Kneib for providing his Lens Tool software for modeling the system, and Lars Freyhammer for performing the observations. We thank Kirsten K. Knudsen and Anja C. Andersen for valuable discussions. IB is supported in part by contract ARC94/99-178 "Action de Recherche Concertée de la Communauté Française (Belgium)" and Pôle d'Attraction Interuniversitaire, P4/05 (SSTC, Belgium). The data presented here have been taken using ALFOSC, which is owned by the Instituto de Astrofisica de Andalucia (IAA) and operated at the Nordic Optical Telescope under agreement between IAA and the Astronomical Observatory of Copenhagen. This work was supported by the Danish Natural Science Research Council (SNF).

References

Bertin E., Arnouts S., 1996, A&AS 117, 393
Burud I., Stabell R., Magain P. et al., 1998, A&A 339, 701
Cardelli J.A., Clayton G.C., Mathis J.S., 1989, ApJ 345, 245
Courbin F., Lidman C., Magain P., 1998, A&A 330, 57
Diplas A., Savage B.D., 1994, ApJ 427, 274
Falco E., Impey C.D., Kochanek C.S. et al., 1999, ApJ 523, 617
Fall S.M., Pei, Y.C. 1993, ApJ 402, 479
Fitzpatrick E.L., 1999, PASP 111, 63
Fukugita M., Shimasaku K., Ichikawa T., 1995, PASP 107, 945
Kneib J.-P., Ellis R.S., Smail I. et al., 1996 ApJ 471, 643
Magain P., Courbin F., Sohy S., 1998, ApJ 494, 452
Malhotra S., Rhoads J.E, Turner E.L., 1997, MNRAS 288, 138
Mathis J.S., 1990, ARA&A 28, 37
Myers S.T., Rusin D., Fassnacht C. D. et al., 1999, AJ 117, 2565
Nadeau D., Yee H. K. C., Forrest W. J. et al., 1991, ApJ 376, 430
Stetson P.B., 1987, PASP 99, 191